Dalton Transactions

An international journal of inorganic chemistry

www.rsc.org/dalton

Volume 41 | Number 39 | 21 October 2012 | Pages 11909–12312

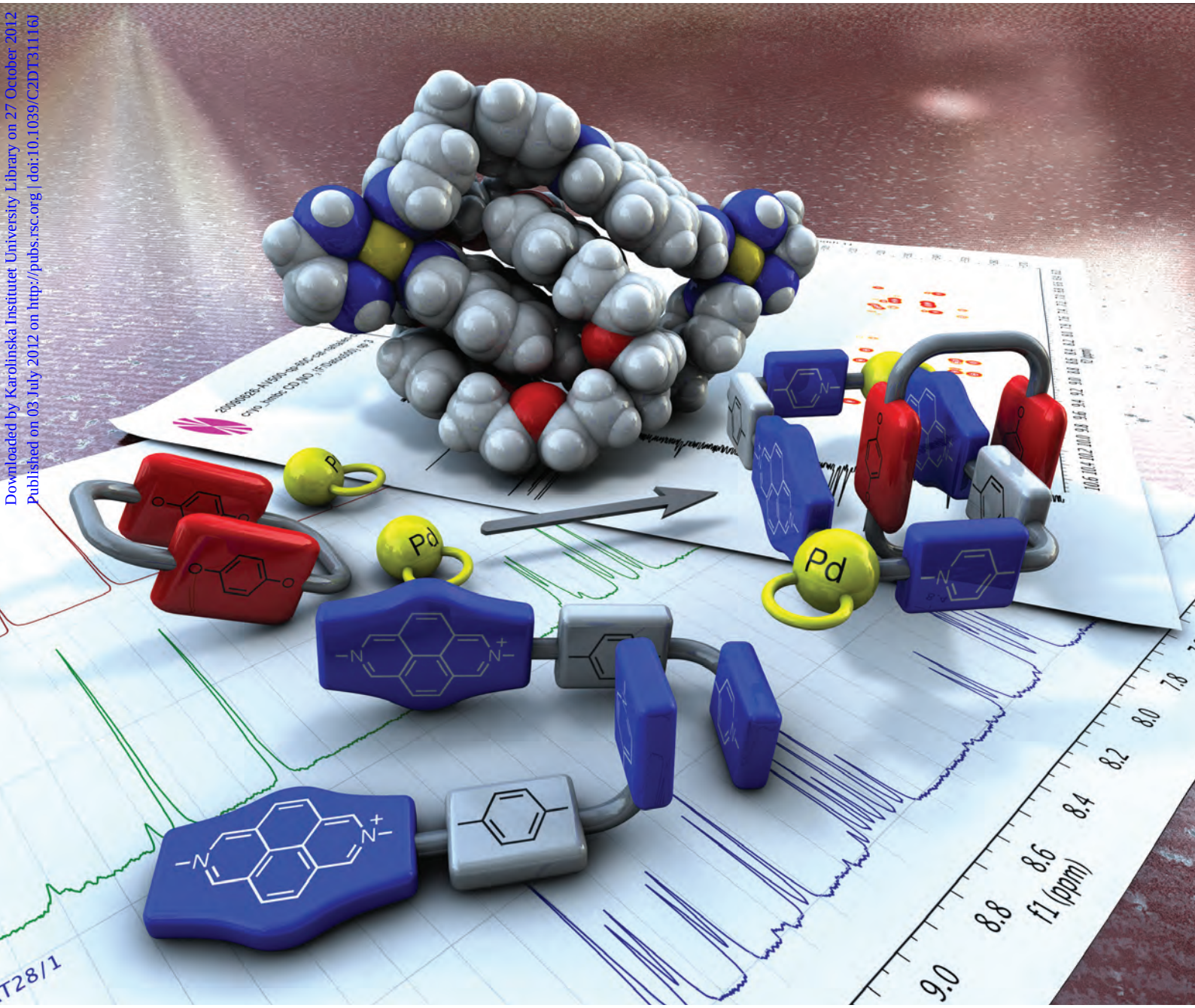

ISSN 1477-9226

RSC Publishing

COVER ARTICLE

Carlos Peinador, José M. Quintela *et al.*

[2]Catenanes and inclusion complexes derived from self-assembled rectangular Pd^{II} and Pt^{II} metallocycles

1477-9226(2012)41:39;1-I

Dalton Transactions

Dynamic Article Links
View Online

Cite this: *Dalton Trans.*, 2012, **41**, 11992

www.rsc.org/dalton

PAPER

[2]Catenanes and inclusion complexes derived from self-assembled rectangular Pd^{II} and Pt^{II} metallocycles†

Cristina Alvariño, Alessio Terenzi,‡ Víctor Blanco,§ Marcos D. García, Carlos Peinador* and José M. Quintela*

Received 23rd May 2012, Accepted 3rd July 2012
DOI: 10.1039/c2dt31116j

New inclusion complexes and [2]catenanes were self-assembled from a fluorescent diazapyrenium based ligand, a Pd^{II} or Pt^{II} complex, and cyclic or acyclic electron rich aromatic guests in aqueous and organic media. The molecular rectangles display a π-deficient cavity suitable to incorporate π-donor aromatic systems. The inclusion complexes between the metallocycles and phenylenic (**2a,b**) and naphthalenic (**3a,b–5a,b**) derivatives were studied by NMR, UV-vis and fluorescence spectroscopy. The crystal structure of (**3b**) ⊂ **1a**·$6PF_6$ confirmed the insertion of the guest into the cavity of the metallocycle. Following the same self-assembly strategy, the use of polyethers **6**,**7** as π-donors resulted in the self-assembly of the [2]catenanes **1a**(**6**,**7**)·$6PF_6$. Single-crystal X-ray analysis of **1a**(**7**)·$6PF_6$ revealed the [2]catenane structure being stabilized by π-stacking and [C–H···O] interactions.

Introduction

Interlocked molecules represent an important group of molecular devices, as potential control over intramolecular motion exerted by external stimuli can be achieved.[1] Among those supramolecules, catenanes, defined as structures composed of two or more interlocked macrocycles, have remained a synthetic challenge for a long time. However, the development of template strategies based on noncovalent interactions promoted and facilitated the preparation of such supramolecules, with many examples of [2]-catenanes being synthesized *via* π-donor/π-acceptor complexes,[2] hydrogen bond interactions,[3] anion templation[4] or metal complexation.[5] In this context, metal-directed self-assembly has proven to be a powerful tool in order to build a great number of 2D and 3D supramolecular structures, including catenanes.[6]

Over the last few years, our research group has developed a self-assembly strategy based on π-deficient *N*-monoalkyl-4,4′-bipyridium or *N*-monoalkyl-2,7-diazapyrenium salts and palladium(II) or platinum(II) complexes. Coordination bonds, π–π stacking interactions, and hydrophobic forces play an important role in the assembly of inclusion complexes, [2] and [3]catenanes, and molecular knots based on these ligands.[7]

Continuing our systematic investigations into Pd^{II}/Pt^{II}-directed self-assembly of supramolecular architectures based on *N*-monoalkyl-2,7-diazapyrenium units, in this paper we report the synthesis of [2]catenanes and inclusion complexes assembled from dinuclear metallocycles **1a,b**. As previously described, these rectangular receptors are able to bind a series of polycyclic aromatic hydrocarbons such as pyrene or triphenylene by insertion of the substrate into the suitable hydrophobic π-deficient cavity of the metallocycle.[8] Thus, the formation of catenanes and inclusion complexes from acyclic or cyclic electron rich aromatic substrates and metallocycles **1a,b** was projected.

Results and discussion

Inclusion of aromatic guests

The complexation process of the Pd^{II}-based metallocycle **1a** with a series of aromatic guests (**2a,b–5a,b**, Fig. 1) was studied by NMR. Addition of 1 equiv. of the corresponding guest to a 2.5 mM solution of **1a**·$6NO_3$ in D_2O produced clear changes in the ^1H NMR spectra. On the one hand, protons of the guest (*e.g.*, **2b**: $\Delta\delta_{Hq} = -1.35$ ppm; **5a**: $\Delta\delta_{Hq} = -2.09$ ppm, $\Delta\delta_{Hr} = -2.70$ ppm, $\Delta\delta_{Hs} = -2.41$ ppm) and protons located on the central part of the phenylene–diazapyrene system of the host (H_c, H_d, H_h, and H_j) are shifted upfield as a consequence of their mutual shielding. On the other hand, hydrogen nuclei of the pyridine ring are shifted to higher frequencies upon complexation, suggesting the occurrence of [C–H···π] interactions with the guest in solution (Table 1). Nevertheless, this shifting to higher frequencies is less important than those observed in previous examples of inclusion complexes of **1a** with polycyclic

Departamento de Química Fundamental, Universidade da Coruña, Campus da Zapateira, Rúa da Fraga 10, 15008 A Coruña, Spain. E-mail: carlos.peinador@udc.es, jose.maria.quintela@udc.es; Fax: +34 981 167065; Tel: +34 981 167000

†Electronic supplementary information (ESI) available: ^1H, ^{13}C, and 2D NMR spectra, ORTEP representations, titration protocols and binding curves, and X-ray crystallographic files (CIF). CCDC 883118 and 883119. For ESI and crystallographic data in CIF or other electronic format see DOI: 10.1039/c2dt31116j

‡Current address: Dip. di Scienze e Tecnologie Molecolari e Biomolecolari (STEMBIO) Università di Palermo, Sezione di Chimica Farmaceutica e Biologica Via Archirafi, 32 – 90123 Palermo (Italy)
§Current address: School of Chemistry, University of Edinburgh, The King's Buildings, West Mains Road, EH9 3JJ, Edinburgh (UK).

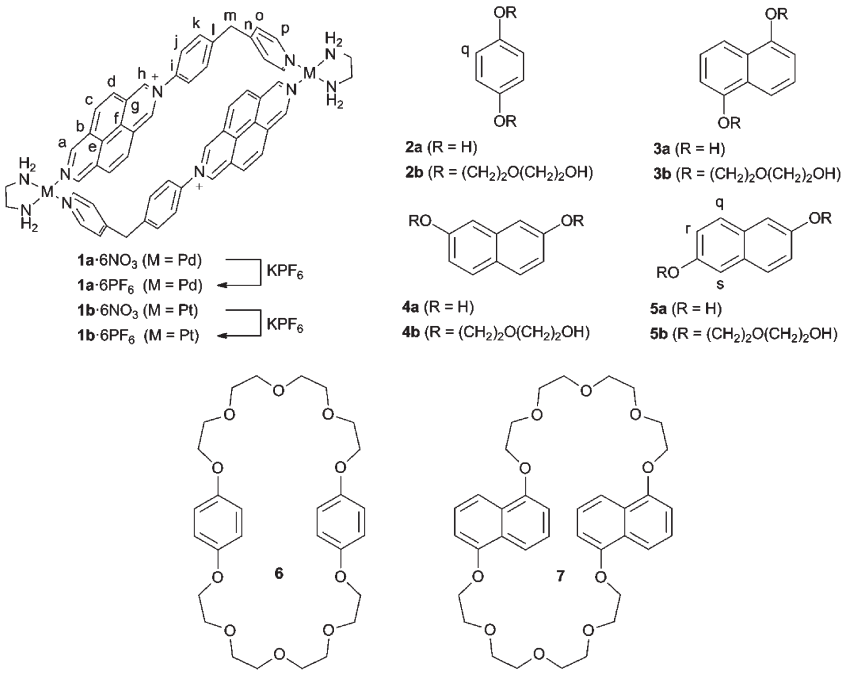

Fig. 1 Pd^{II} and Pt^{II} self-assembled macrocyclic hosts, aromatic guests and crown ethers used in this work.

aromatic hydrocarbons,[8b] suggesting that in this system the [C–H···π] interactions are less important due to the shorter length of guests **2a,b–5a,b** with respect to those.

In order to obtain further insight into the binding mode of metallocycles **1a,b** and the phenylenic/naphthalenic derivatives **2a,b–5a,b** in organic and aqueous environments, UV-vis and fluorescence spectroscopies were used to study the complexation processes between the Pt^{II}-based metallocycle **1b** and substrates **2a** and **3b**. In nitromethane, the UV-vis spectra of the inclusion complexes showed the presence of charge-transfer absorption bands, which were used to determine the stoichiometry and binding constants between **1b**·$6PF_6$ and **2a**/**3b** using the dilution method. Job's plots showed the maximal complexation at a 0.5 molar fraction of host **1b**·$6PF_6$ and guests **2a** or **3b**. The higher K_a value for **3b** ($K_a = 8477 \pm 1253\ M^{-1}$) in comparison with **2a** ($K_a = 386 \pm 21\ M^{-1}$) can be attributed to the best fitting of the naphthalene moiety inside the internal cavity of the host, as well as the hydrogen bonding interactions between the polyether chains of the host and metallocyclic protons. DOSY experiments in D_2O performed with the Pd^{II}-based metallocycle **1a** are in agreement with the relative binding affinities between the host and the phenylenic/naphthalenic guests. In (**4b**) ⊂ **1a**·$6NO_3$ the signals of **4b** show a similar diffusion coefficient to those of **1a**, indicating a stronger binding than that observed in (**2b**) ⊂ **1a**·$6NO_3$, where the signals of the hydroquinone derivative **2b** exhibit a significantly larger diffusion coefficient than those belonging to the host (see ESI†).

X-ray diffraction analysis of red single crystals of inclusion complex (**3b**) ⊂ **1a**·$6PF_6$, obtained by slow diffusion of diethyl ether into a solution of **1a**·$6PF_6$ and **3b** in nitromethane, revealed the complex being stabilized by [C–H···O] hydrogen bonds between α-CH diazapyrenium protons on the host and oxygen atoms of the polyether chain of the guest (Fig. 2 and Table 2). The interplanar distance between the naphthalene moiety and the diazapyrene system is 3.30 Å, maximizing the π–π interactions in the supramolecular species. The relative position of the guest within the host cavity, placed in front of the diazapyrene moiety and with a torsion angle of 39° between this system and the phenylene ring, suggests this aromatic ring of the host not being implicated in π–π interactions. The absence of [C–H···π] contacts between aromatic protons of the guest and the pyridine rings on the shorter side of the rectangle, observed in similar systems,[9] can be attributed to the larger side of the host (14.86 Å) when compared with previously reported metallocycles (11.07–10.45 Å).[10] As expected, the Pd–N bond distances ranged from 2.02 Å to 2.04 Å, while the N(Py)–Pd–N(Py) angle is 89° close to the ideal square planar geometry.

In order to study the complexation process between **1b** and **3b** in H_2O, we decided to take advantage of the fluorescent nature of **1b**·$6NO_3$. In H_2O, the Pt^{II} metallocycle shows two intense structured absorption bands corresponding to electronic transitions to the first and second ππ* excited states (see ESI†), as is typical for diazapyrenium-containing ligands and metallocycles.[9a,12] Upon irradiation at λ_{exc} = 326 nm in H_2O, it displays a fluorescence band at room temperature (λ_{max} = 439 nm). Addition of aliquots of **3b** in water resulted in a significant quenching of the above-mentioned band, as an expected result of the π-donor–π-acceptor interactions upon complexation.[12]

As shown in Fig. 3, the data resulting from the corresponding titration experiment using **1b**·$6NO_3$ as a fluorophore and **3b** as a quencher were perfectly adjusted to a 1 : 1 binding isotherm[13] ($K_a = 4.4 \times 10^5 \pm 1.8 \times 10^4$), being well adjusted as well to a linear model in the Stern–Volmer plot ($K_{sv} = 1.55 \times 10^5 \pm 2 \times 10^3\ M^{-1}$, see ESI† for further details). The similarity between K_a and K_{sv}, being on the same order of magnitude, suggests that the quenching mechanism is predominantly static and therefore linked to the complexation event.

Table 1 ^{1}H and ^{13}C NMR chemical shift data ($\Delta\delta$) for inclusion complexes (**2a,b–5a,b**) ⊂ **1a**·6NO_3 (2.5 mM, D_2O) and catenanes **1a**(**6,7**)·6PF_6 (5.0 mM, CD_3NO_2)[a]

		a	b	c	d	e	f	g	h	i	j	k	l	m	n	o	p
(**2a**) ⊂ **1a**·6NO_3 [b]	^{1}H	0.08		−0.02	−0.10				−0.21		−0.12	0.02		−0.02		0.06	0.08
	^{13}C	0.04	−0.18	0.05	−0.13	−0.21	−0.59	−0.16	−0.92	−0.61	−0.41	0.11	−0.03	0.06	0.07	0.02	−0.02
(**3a**) ⊂ **1a**·6NO_3 [b]	^{1}H	0.05		−0.15	−0.35				−0.62		−0.15	0.06		0.06		0.15	0.15
	^{13}C	−0.15	−0.70	−0.35	−0.18	*d*	−1.44	−0.51	−2.03	−1.28	−0.50	0.11	0.32	0.09	0.76	0.09	0.07
(**4a**) ⊂ **1a**·6NO_3 [b]	^{1}H	0.08		−0.08	−0.31				−0.60		−0.16	0.07		0.01		0.09	0.10
	^{13}C	−0.05	−0.65	−0.21	−0.18	−0.57	−1.34	−0.50	−2.37	−1.47	−0.69	0.15	0.17	0.05	0.45	0.02	−0.04
(**5a**) ⊂ **1a**·6NO_3 [b]	^{1}H	0.07		−0.04	−0.21				−0.44		−0.12	0.06		0.01		0.07	0.08
	^{13}C	0.04	−0.50	−0.09	−0.12	−0.32	−2.14	−0.30	−1.76	−1.12	−0.57	0.13	0.10	0.05	0.24	0.03	−0.04
1a(**6**)·6PF_6 [c]	^{1}H	0.01		−0.31	−0.32				0.06		0.21	0.12		0.05		0.08	0.06
		−0.16		−0.01	−0.20				−0.63		−0.08	0.16		0.00		0.08	0.19
	^{13}C	0.19	*d*	−0.30	−0.21	*d*	*d*	*d*	0.06	−0.19	0.65	−0.04	−0.19	0.24	0.49	0.11	0.04
		−0.17	*d*	0.03	0.11	*d*	*d*	*d*	−0.98	−0.51	−0.28	0.52	0.44	0.15	0.30	−0.18	0.60

[a] Hydrogen and carbon labels (a–p) are defined in Fig. 1. [b] The δ values are compared to those of metallocycle **1a**·6NO_3. [c] The δ values are compared to those of metallocycle **1a**·6PF_6. [d] Not assigned.

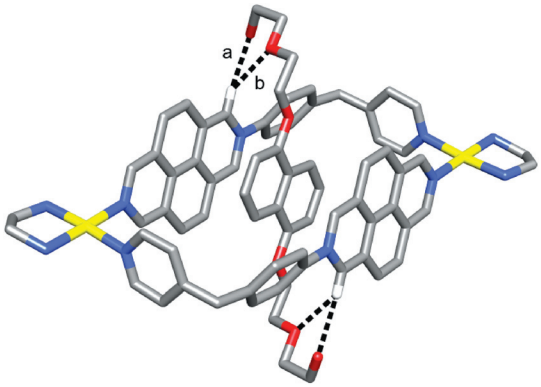

Fig. 2 Crystal structure of (**3b**) ⊂ **1a**·6PF_6 showing [C–H···O] hydrogen bonds. [H···O] and [C···O] distances and [C–H···O] angles: a 2.64, 3.54 Å, 159°; a′ 2.29, 3.22 Å, 167°;[11] b 2.78, 3.48 Å, 132°. Solvent molecules, counterions and remaining hydrogen atoms are omitted for clarity. Colour scheme: C, grey; O, red; N, blue; H, white; Pd, yellow.

Table 2 X-ray crystallographic experimental and refinement data for (**3b**) ⊂ **1a**·6PF_6 and **1a**(**7**)·6PF_6[a]

	(**3b**) ⊂ **1a**·6PF_6	**1a**(**7**)·6PF_6
Chemical formula	$C_{78}H_{88}F_{36}N_{14}O_{14}P_6Pd_2$	$C_{192}H_{216}F_{72}N_{28}O_{36}P_{12}Pd_4$
Formula mass	2560.24	5657.17
Crystal system	Triclinic	Monoclinic
Space group	$P\bar{1}$	Cc
a/Å	12.1541(4)	30.8974(9)
b/Å	14.5559(5)	21.7294(6)
c/Å	17.0550(5)	20.8416(6)
α/°	81.470(2)	90
β/°	73.532(2)	118.4017(15)
γ/°	66.056(2)	90
V/Å^3	2642.58(15)	12308.4(7)
Temperature/K	100(2)	100(2)
Z	1	2
D_{calc}/Mg m^{-3}	1.589	1.526
μ/mm^{-1}	0.557	0.490
F(000)	1272	5728
θ limits	1.53 to 28.37°	2.33 to 28.38°
hkl limits	−16, 16/−19, 19/−22, 22	−41, 41/−29, 29/−27, 27
No. of reflections measured	69 366	81 414
No. of independent reflections	13 029	29 395
R_{int}	0.0413	0.0423
$R(I > 2\sigma(I))$	R_1 = 0.0774 wR_2 = 0.2220	R_1 = 0.0909 wR_2 = 0.2375
R (all data)	R_1 = 0.0953 wR_2 = 0.2395	R_1 = 0.1244 wR_2 = 0.2778
Goodness of fit on F^2	0.882	1.050

[a] In common: refinement method, full-matrix least-squares on F^2. Wavelength 0.71073 Å (Mo-Kα), temperature 100(2) K. Absorption correction method: multi-scan.

Self-assembly of [2]catenanes

In principle, the formation of [2]catenanes with dioxoaryl cyclophanes (**6** and **7**) should be favored by (a) π–π interactions between *N*-monoalkyl-2,7-diazapyrenium systems and dioxoaryl rings and (b) hydrogen bonds between hydrogens of the ligand

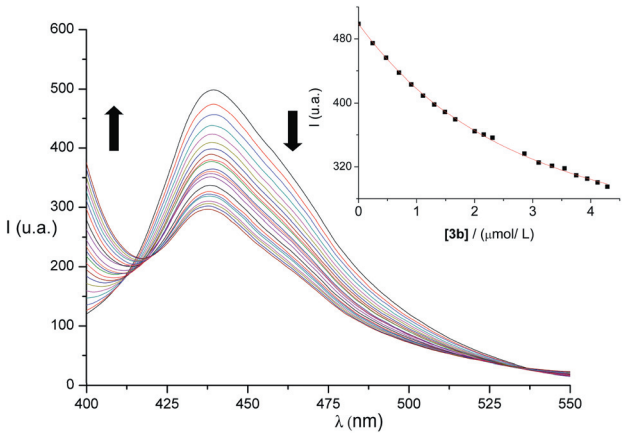

Fig. 3 Fluorescence spectra (H_2O, 293 K, λ_{exc} = 326 nm) of a solution of **1b**·6NO_3 (1.0×10^{-6} M) after successive addition of aliquots of a solution of guest **3b** (1.0×10^{-5} M) and host **1b**·6NO_3 (1.0×10^{-6} M). Inset: emission intensity at λ_{max} = 439 nm *vs.* concentration of **3b** fitted to a 1 : 1 isotherm.

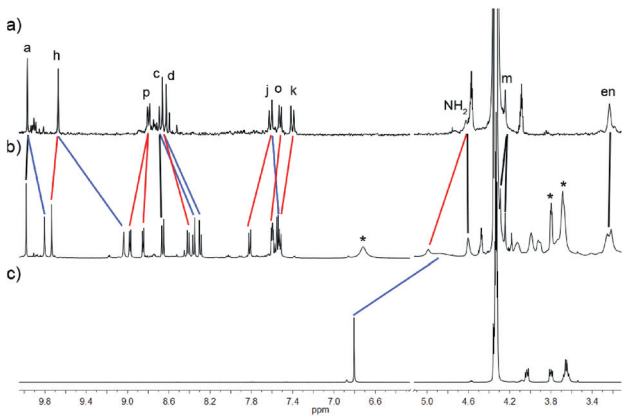

Fig. 4 ^{1}H NMR (500 MHz, CD_3NO_2, 298 K) spectra of (a) metallocycle **1a**·6PF_6; (b) catenane **1a**(**6**)·6PF_6; (c) cyclophane **6**. Labels are defined in Fig. 1. *Signals corresponding to excess of **6**.

and oxygen atoms from the cyclophanes, as has been observed in similar systems.[14]

With those presumptions in mind, the self-assembly of [2]-catenanes derived from metallocycle **1a** was carried out in CD_3NO_2. The addition of 1 equiv. of **6** to a 5 mM solution of metallocycle **1a**·6PF_6 induced changes in the ^{1}H NMR spectrum compatible with the formation of the [2]catenane (Fig. 4). In the [2]catenane, exchange between the "inside" and "alongside" hydroquinol rings is fast, resulting in a broad average signal at δ = 4.87 ppm. When an excess of cyclophane **6** is added a new resonance at 6.72 ppm, corresponding to the aromatic protons of free **6**, was detected. Moreover, this signal at 6.72 ppm showed a higher diffusion coefficient than that corresponding to the signals of the catenane (*i.e.* the aromatic signals of **1a** and the methylene groups on the polyether chains of **6**) in the DOSY experiment. Conversely, exchange between the "inside" and "alongside" diazapyrene systems is slow, resulting in two different sets of signals for the diazapyrene moieties but also the phenylene and pyridyl units (Fig. 4 and Table 1). The kinetic lability of the Pd–N(Py) bond at room temperature allowed the catenation process under thermodynamic control, all the species being in equilibrium.

A careful inspection of the ^{1}H, ^{13}C and 2D NMR spectra of catenane **1a**(**7**)·6PF_6 revealed similar characteristics to those of the catenane with **6**. Again the expected slow exchange between $DIAZ_{in}$ and $DIAZ_{out}$ in the NMR timescale was observed. This resulted in the presence of two sets of signals for the protons and carbons of the phenylene and pyridine rings and ethylenediamine units of the metallocycle. However, only three resonances (H_a, H_c and H_d) were identified in the ^{1}H NMR spectrum for the diazapyrenium moieties. These signals probably correspond to $DIAZ_{out}$, being H_h, and the signals for the protons of $DIAZ_{in}$ broaden due to the interaction with the inside naphthalene unit of the cyclophane, and the manifestation of different equilibria related to possible different insertion modes of the naphthalene moiety within the cavity. This resulted also in the aromatic protons of **7** not being detected in the ^{1}H NMR.

Nonetheless, single crystals of catenane **1a**(**7**)·6PF_6, suitable for single crystal X-ray crystallography, were obtained by slow diffusion of diethyl ether into a solution of ligand **1a**·6PF_6 and **7** in nitromethane (Table 2). As shown in Fig. 5, the solid state structure displays the expected [2]catenane with the hexacationic metallocycle, interlocked by one molecule of cyclophane with a parallel π-stacking disposition of four aromatic systems. The distance between the diazapyrene systems is *ca.* 7.2 Å, and the interplanar separation between the inside diazapyrene and the alongside naphthalene is *ca.* 3.3 Å. Additional stabilization is achieved by hydrogen bonding between oxygen atoms of the polyether chain and hydrogens of the diazapyrene moiety. The N–Pd bond distances and the N(Py)–Pd–N(Py) angle exhibit the usual values (2.00–2.04 Å and 89°, respectively). As in the case of the inclusion complex (**3b**) ⊂ **1a**, the phenylene and diazapyrene systems are not coplanar, the dihedral angle being 43°. As is typical in these kinds of systems, the structure is

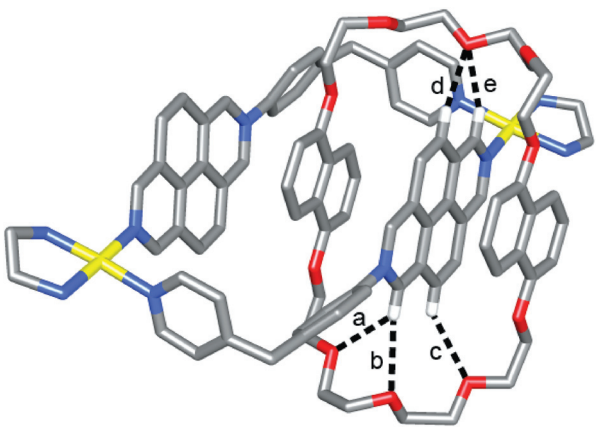

Fig. 5 Stick representation of the solid state structure of catenane **1a**(**7**)·6PF_6 showing [C–H···O] hydrogen bonds. [H···O] and [C···O] distances and [C–H···O] angles: a 2.71, 3.40 Å, 130°; b 2.68, 3.61 Å, 167°; c 2.77, 3.52 Å, 135°; d 2.39, 3.28 Å, 156°; e 2.79, 3.59 Å, 143°. Solvent molecules, counterions and remaining hydrogen atoms are omitted for clarity. Colour scheme: C, grey; O, red; N, blue; H, white; Pd, yellow.

stabilized as well by means of [C–H···O] hydrogen bonds between oxygen atoms of the polyether chains on the cyclophane and hydrogens in the α position of the diazapyrene unit. Interestingly, no [C–H···O] interactions are observed between the polyether chains and the NH_2 groups of the ethylenediamine units. Instead, short contacts to the hydrogens in the γ position (less acidic than those next to the N) were detected.

Conclusions

Based on the known tendency of the diazapyrenium-based Pd^{II}/Pt^{II} metallocycles **1a,b** to produce inclusion complexes with electron rich aromatic substrates, we have investigated the self-assembly of inclusion complexes and [2]catenanes derived from those dinuclear rectangular-shaped coordination complexes. The cavity of these metallocycles is suitable for the binding of phenylenic and naphthalenic derivatives, with association constants in good agreement with the nature of the guests and the reaction media. The solid state structure of the inclusion complex (**3b**) ⊂ **1a**·6PF_6 shows stabilizing interactions by means of π-stacking between the naphthalenic core of the host and the diazapyrenium moieties of the guest, as well as hydrogen bonding between oxygen atoms on the aliphatic chains in **3** and hydrogen atoms on the metallocycle. By using the same metal-directed self-assembly strategy, dinuclear Pd^{II} [2]catenanes **1a**(**6**,**7**)·6PF_6 were successfully synthesised and characterised by means of NMR spectroscopy and single crystal X-ray crystallography (for **1a**(**7**)·6PF_6).

Experimental section

General methods

Metallocycles **1a,b**·6X (X = NO_3, PF_6),[8b,15] guests **2b**,[16] **3b**,[17] **4b**[18] and **5b**,[19] and cyclophanes **6**[17] and **7**[19] were prepared according to literature procedures. All other reagents used were commercial grade chemicals from freshly opened containers. Milli-Q water was purified with a Millipore Gradient A10 apparatus. Proton and carbon nuclear magnetic resonance spectra were recorded on a Bruker Avance 300 spectrometer or a Bruker Avance 500 spectrometer equipped with a dual cryoprobe for ^1H and ^{13}C, using the deuterated solvent as a lock and the residual protiated solvent as an internal standard. DOSY experiments were referenced using the value 1.92×10^{-9} m^2 s^{-1} for the DHO signal in D_2O at 298 K[20] and the value 1.97×10^{-9} m^2 s^{-1} for the CHD_2NO_2 signal in CD_3NO_2 at 298 K.[21] UV-vis spectra were recorded on a Jasco V-650 spectrometer. Fluorescence spectra were recorded at room temperature on a Perkin Elmer L550B fluorescence spectrometer, using a 290 nm cut-off filter with a slit of 15 nm.

Crystal structure analysis

X-ray diffraction quality crystals were grown by slow diffusion of diethyl ether into solutions of (**3b**) ⊂ **1a**·6PF_6 and **1a**(**7**)·6PF_6 in nitromethane. The X-ray diffraction data were collected on a Bruker X8 APEXII. The structure was solved by direct methods and refined with the full-matrix least-squares procedure (SHELX-97)[22] against F^2 using the WinGX software.[23] Hydrogen atoms were placed in idealized positions with $U_{eg}(H) = 1.2U_{eg}(C)$ and were allowed to ride on their parent atoms. The crystal lattice of the crystal of (**3b**) ⊂ **1a**·6PF_6 contains a void filled with scattered electron density. Attempts to model this density were unsuccessful, and therefore the SQUEEZE protocol inside PLATON[24] was used to remove the void electron density. The analysis of the scattered density performed shows a void of 294.6 $Å^3$ and 62 electrons, suggesting the presence of two disordered molecules of nitromethane (64 electrons). The crystallographic data for (**3b**) ⊂ **1a**·6PF_6 (CCDC 883118) and **1a**(**7**)·6PF_6 (CCDC 883119) have been deposited at the Cambridge Crystallographic Data Centre.

General method for the inclusion of aromatic guests

To a solution of **1a**·6NO_3 (5.0×10^{-3} mmol) in D_2O (2.0 mL) the corresponding guest **2a,b–5a,b** (5.0×10^{-3} mmol) was added.

Inclusion complex (2a) ⊂ 1a·6NO_3. ^1H NMR (500 MHz, D_2O) δ: 10.00 (s, 4H), 9.48 (s, 4H), 8.83 (d, J = 6.8 Hz, 4H), 8.56 (d, J = 9.2 Hz, 4H), 8.38 (d, J = 9.2 Hz, 4H), 7.54 (d, J = 6.8 Hz, 4H), 7.39 (d, J = 8.8 Hz, 4H), 7.36 (d, J = 8.8 Hz, 4H), 6.01 (s, 12H), 4.12 (s, 4H), 3.01 (s, 8H). ^{13}C NMR (125 MHz, D_2O) δ: 155.18 (C), 150.88 (CH), 148.14 (CH), 142.77 (C), 141.19 (C), 138.08 (CH), 130.71 (CH), 129.85 (CH), 128.62 (C), 128.34 (C), 127.97 (CH), 127.32 (CH), 126.85 (C), 124.91 (C), 124.39 (CH), 46.86 (CH_2), 46.77 (CH_2), 39.93 (CH_2).

Inclusion complex (2b) ⊂ 1a·6NO_3. ^1H NMR (500 MHz, D_2O) δ: 9.99 (s, 4H), 9.50 (s, 4H), 8.85 (d, J = 6.7 Hz, 4H), 8.60 (d, J = 9.2 Hz, 4H), 8.42 (d, J = 9.2 Hz, 4H), 7.61 (d, J = 6.8 Hz, 4H), 7.50 (d, J = 8.8 Hz, 4H), 7.47 (d, J = 8.7 Hz, 4H), 5.65 (s, 4H), 4.19 (s, 4H), 3.78 (m, 4H), 3.58 (m, 4H), 3.44 (br, 4H), 3.29 (br, 4H), 3.02 (s, 8H). ^{13}C NMR (125 MHz, D_2O) δ: 155.47 (C), 151.06 (CH), 150.96 (C), 148.24 (CH), 143.18 (C), 141.35 (C), 138.43 (CH), 130.82 (CH), 129.94 (CH), 128.58 (C), 128.20 (C), 128.16 (C), 127.48 (C), 126.75 (C), 124.66 (CH), 114.19 (CH), 71.88 (CH_2), 68.68 (CH_2), 66.99 (CH_2), 60.40 (CH_2), 46.92 (CH_2), 46.81 (CH_2), 39.87 (CH_2).

Inclusion complex (3a) ⊂ 1a·6NO_3. ^1H NMR (500 MHz, D_2O) δ: 9.97 (s, 4H), 9.07 (s, 4H), 8.90 (d, J = 6.8 Hz, 4H), 8.43 (d, J = 9.2 Hz, 4H), 8.13 (d, J = 9.2 Hz, 4H), 7.63 (d, J = 6.9 Hz, 4H), 7.43 (t, J = 12.8 Hz, 4H), 7.33 (d, J = 8.6 Hz, 4H), 5.59 (br, 2H), 5.37 (br, 4H), 4.18 (s, 4H), 3.01 (m, 8H). ^{13}C NMR (125 MHz, D_2O) δ: 155.87 (C), 150.97 (CH), 147.95 (CH), 143.12 (C), 140.52 (C), 136.97 (CH), 130.71 (CH), 129.46 (CH), 128.15 (C), 128.01 (C), 127.92 (CH), 127.39 (CH), 126.06 (C), 124.30 (CH), 111.31 (CH), 107.54 (CH), 46.89 (CH_2), 46.78 (CH_2), 39.96 (CH_2).

Inclusion complex (3b) ⊂ 1a·6NO_3. ^1H NMR (500 MHz, D_2O) δ: 9.98 (br, 4H), 9.50 (br, 4H), 8.92 (d, J = 6.7 Hz, 4H), 8.48 (br, 4H), 7.67 (t, J = 9.8 Hz, 4H), 7.52 (d, J = 8.5 Hz, 4H), 7.44 (d, J = 8.6 Hz, 4H), 5.36 (br, 4H), 4.23 (s, 4H), 3.97–3.74 (br, 16H), 3.01 (m, 8H). ^{13}C NMR (125 MHz, D_2O) δ: 156.22 (C), 151.06 (CH), 148.03 (CH), 143.50 (C), 140.54 (C), 136.93

(CH), 130.72 (CH), 129.62 (CH), 128.01 (C), 127.97 (C), 127.38 (CH), 125.87 (C), 124.53 (CH), 124.24 (C), 72.24 (CH_2), 69.22 (CH_2), 60.58 (CH_2), 46.93 (CH_2), 46.80 (CH_2), 39.95 (CH_2).

Inclusion complex (4a) ⊂ 1a·6NO$_3$. ^{1}H NMR (500 MHz, D_2O) δ: 10.00 (s, 4H), 9.09 (s, 4H), 8.85 (d, J = 6.9 Hz, 4H), 8.50 (d, J = 9.2 Hz, 4H), 8.17 (d, J = 9.2 Hz, 4H), 7.57 (d, J = 6.9 Hz, 4H), 7.44 (d, J = 8.6 Hz, 4H), 7.32 (d, J = 8.7 Hz, 4H), 6.04 (br, 2H), 5.31 (br, 2H), 4.15 (s, 4H), 3.01 (s, 8H). ^{13}C NMR (125 MHz, D_2O) δ: 155.56 (C), 152.72 (C), 150.86 (CH), 148.05 (CH), 142.97 (C), 140.33 (C), 136.63 (CH), 130.75 (CH), 129.59 (CH), 128.15 (C), 128.00 (C), 127.92 (CH), 127.60 (CH), 127.32 (CH), 126.10 (C), 124.55 (C), 124.11 (CH), 113.57 (CH), 105.55 (CH), 46.87 (CH_2), 46.77 (CH_2), 39.92 (CH_2).

Inclusion complex (4b) ⊂ 1a·6NO$_3$. ^{1}H NMR (500 MHz, D_2O) δ: 10.07 (s, 4H), 9.15 (s, 4H), 8.94 (d, J = 6.7 Hz, 4H), 8.54 (d, J = 9.2 Hz, 4H), 8.21 (d, J = 9.1 Hz, 4H), 7.67 (d, J = 6.7 Hz, 4H), 7.47 (d, J = 8.5 Hz, 4H), 7.33 (d, J = 8.2 Hz, 4H), 4.19 (s, 4H), 4.00 (m, 4H), 3.85 (m, 4H), 3.56 (br, 4H), 3.39 (br, 4H), 3.02 (m, 8H). ^{13}C NMR (125 MHz, D_2O) δ: 155.74 (C), 154.94 (C), 151.02 (CH), 148.23 (CH), 143.17 (C), 140.47 (C), 137.09 (CH), 130.84 (CH), 129.74 (CH), 128.12 (C), 128.08 (C), 127.98 (CH), 127.50 (CH), 126.89, 126.22 (C), 124.40 (C), 124.18 (CH), 113.94 (CH), 104.34 (CH), 72.24 (CH_2), 68.86 (CH_2), 66.16 (CH_2), 60.74 (CH_2), 46.94 (CH_2), 46.82 (CH_2), 39.85 (CH_2).

Inclusion complex (5a) ⊂ 1a·6NO$_3$. ^{1}H NMR (500 MHz, D_2O) δ: 9.99 (s, 4H), 9.25 (br s, 4H), 8.83 (d, J = 6.5 Hz, 4H), 8.54 (d, J = 9.2 Hz, 4H), 8.27 (d, J = 8.6 Hz, 4H), 7.55 (d, J = 6.6 Hz, 4H), 7.43 (d, J = 8.5 Hz, 4H), 7.36 (d, J = 8.3 Hz, 4H), 5.64 (d, J = 8.7 Hz, 2H), 4.84 (s, 2H), 4.48 (d, J = 7.2 Hz, 2H), 4.15 (s, 4H), 3.01 (m, 8H). ^{13}C NMR (125 MHz, D_2O) δ: 155.35 (C), 150.86 (CH), 149.92 (C), 148.14 (CH), 142.90 (CH), 140.68 (C), 137.24 (CH), 130.73 (CH), 129.71 (CH), 128.26 (C), 127.98 (CH), 127.33 (CH), 125.59 (C), 125.31 (CH), 124.78 (C), 124.23 (CH), 116.27 (CH), 106.36 (CH), 46.86 (CH_2), 46.75 (CH_2), 39.92 (CH_2).

Inclusion complex (5b) ⊂ 1a·6NO$_3$. ^{1}H NMR (500 MHz, D_2O) δ: 10.05 (br s, 4H), 9.41 (br, 4H), 8.88 (d, J = 6.1 Hz, 4H), 8.55 (br, 4H), 8.25 (br, 4H), 7.67 (d, J = 6.0 Hz, 4H), 7.51 (t, J = 8.2 Hz, 4H), 7.43 (d, J = 8.6 Hz, 4H), 5.65 (d, J = 8.6 Hz, 2H), 5.53 (s, 2H), 4.20 (s, 4H), 4.07 (m, 4H), 3.91 (m, 4H), 3.76 (br, 4H), 3.48 (br, 2H), 3.23 (br, 4H), 3.01 (m, 8H). ^{13}C NMR (125 MHz, D_2O) δ: 155.89 (C), 152.42 (C), 151.04 (CH), 148.25 (CH), 143.43 (C), 140.47 (C), 136.90 (CH), 130.83 (CH), 129.82 (CH), 128.10 (C), 127.98 (CH), 127.43 (CH), 126.24 (CH), 126.12 (C), 124.36 (CH), 116.05 (CH), 103.90 (CH), 72.28 (CH_2), 69.10 (CH_2), 66.14 (CH_2), 60.84 (CH_2), 46.92 (CH_2), 46.78 (CH_2), 39.90 (CH_2).

General method for the self-assembly of catenanes

To a solution of **1a**·6PF_6 (0.010 mmol) in CD_3NO_2 (2.0 mL) the corresponding cyclophane **6** or **7** (0.010 mmol) was added and the mixture was stirred at 60 °C for 1 h.

Catenane 1a(6)·6PF$_6$. ^{1}H NMR (500 MHz, CD_3NO_2) δ: 9.98 (s, 2H), 9.81 (s, 2H), 9.73 (s, 2H), 9.04 (s, 2H), 8.98 (d, J = 6.8 Hz, 2H), 8.85 (d, J = 6.8 Hz, 2H), 8.66 (d, J = 9.2 Hz, 2H), 8.41 (d, J = 9.1 Hz, 2H), 8.36 (d, J = 9.1 Hz, 2H), 8.29 (d, J = 9.1 Hz, 2H), 7.82 (d, J = 8.6 Hz, 2H), 7.61–7.58 (m, 4H), 7.56 (d, J = 8.8 Hz, 2H), 7.53 (d, J = 8.7 Hz, 2H), 7.52 (d, J = 8.5 Hz, 2H), 6.72 (br s, 4H), 4.99 (br s, 4H), 4.85 (br, 4H), 4.60 (s, 4H), 4.29 (s, 2H), 4.24 (s, 2H), 4.13 (m, 4H), 3.99 (m, 4H), 3.91 (m, 4H), 3.80 (m, 8H), 3.69 (m, 16H), 3.24 (m, 8H). ^{13}C NMR (125 MHz, CD_3NO_2) δ: 157.17 (C), 156.98 (C), 153.49 (CH), 152.93 (CH), 151.57 (C), 150.36 (CH), 150.00 (CH), 145.28 (C), 144.65 (C), 143.32 (C), 143.00 (C), 140.57 (CH), 139.53 (CH), 132.79 (CH), 132.23 (CH), 131.72 (CH), 131.39 (CH), 130.38 (C), 129.99 (CH), 129.81 (C), 129.67 (C), 129.53 (CH), 129.30 (CH), 129.16 (C), 129.01 (CH), 128.46 (C), 127.72 (C), 126.96 (CH), 126.11 (C), 126.03 (CH), 125.18 (C), 116.44 (CH), 113.81 (CH), 71.63 (CH_2), 71.58 (CH_2), 71.39 (CH_2), 70.81 (CH_2), 70.34 (CH_2), 69.34 (CH_2), 68.07 (CH_2), 49.32 (CH_2), 49.08 (CH_2), 48.86 (CH_2), 48.72 (CH_2), 41.32 (CH_2), 41.23 (CH_2).

Catenane 1a(7)·6PF$_6$. ^{1}H NMR (500 MHz, CD_3NO_2) δ: 9.84 (s, 2H), 9.07 (d, J = 6.7 Hz, 2H), 8.84 (d, J = 6.8 Hz, 2H), 8.57 (br d, J = 8.7 Hz, 2H), 8.19 (br d, J = 7.6 Hz, 2H), 7.79 (d, J = 6.9 Hz, 2H), 7.74 (d, J = 8.6 Hz, 2H), 7.60 (m, 4H), 7.52 (d, J = 8.5 Hz, 2H), 7.22 (d, J = 8.5 Hz, 2H), 4.58 (br s, 4H), 4.32 (s, 2H); 4.24 (s, 2H), 4.07–3.70 (m, 24H), 3.29–3.19 (m, 8H). ^{13}C NMR (125 MHz, CD_3NO_2) δ: 157.88 (C), 157.48 (C), 153.11 (CH), 152.94 (CH), 150.08 (CH), 149.27 (CH), 145.03 (C), 144.86 (C), 142.61 (C), 142.24 (C), 138.06 (CH), 132.35 (CH), 132.13 (CH), 131.50 (C), 130.90 (C), 129.86 (C), 129.69 (C), 129.51 (CH), 129.23 (CH), 129.18 (C), 128.69 (CH), 127.79 (C), 126.57 (CH), 126.23 (C), 125.94 (CH), 125.84 (C), 124.33 (CH), 105.65 (CH), 72.19 (CH_2), 72.07 (CH_2), 71.88 (CH_2), 70.89 (CH_2), 69.38 (CH_2), 49.21 (CH_2), 49.02 (CH_2), 48.81 (CH_2), 41.62 (CH_2), 41.21 (CH_2).

Acknowledgements

This research was supported by Ministerio de Ciencia e Innovación and FEDER (CTQ2010-16484/BQU).

Notes and references

1 (*a*) E. R. Kay, D. A. Leigh and F. Zerbetto, *Angew. Chem., Int. Ed.*, 2007, **46**, 72; (*b*) L. Fang, M. Hmadeh, J. Wu, M. A. Olson, J. M. Spruell, A. Trabolsi, Y.-W. Yang, M. Elhabiri, A.-M. Albrecht-Gary and J. F. Stoddart, *J. Am. Chem. Soc.*, 2009, **131**, 7126; (*c*) A. Coskun, P. J. Wesson, R. Klajn, A. Trabolsi, L. Fang, M. A. Olson, S. K. Dey, B. A. Grzybowski and J. F. Stoddart, *J. Am. Chem. Soc.*, 2010, **132**, 4310.

2 (*a*) G. Barin, A. Coskun, M. M. G. Fouda and J. F. Stoddart, *ChemPlusChem*, 2012, **77**, 159; (*b*) V. Balzani, A. Credi, S. J. Langford, F. M. Raymo, J. F. Stoddart and M. Venturi, *J. Am. Chem. Soc.*, 2000, **122**, 3542; (*c*) H.-R. Tseng, S. A. Vignon, P. C. Celestre, J. Perkins, J. O. Jeppesen, A. Di Fabio, R. Ballardini, M. T. Gandolfi, M. Venturi, V. Balzani and J. F. Stoddart, *Chem.–Eur. J.*, 2004, **10**, 155 and references therein.

3 (*a*) D. A. Leigh, A. Venturini, A. J. Wilson, J. K. Y. Wong and F. Zerbetto, *Chem.–Eur. J.*, 2004, **10**, 4960; (*b*) A. G. Johnston, D. A. Leigh, R. J. Pritchard and M. D. Deegan, *Angew. Chem., Int. Ed.*, 1995, **34**, 1209; (*c*) C. A. Fustin, C. Bailly, G. J. Clarkson, P. De Groote, T. H. Galow, D. A. Leigh, D. Robertson, A. M. Z. Slawin and

J. K. Y. Wong, *J. Am. Chem. Soc.*, 2003, **125**, 2200; (*d*) R. Jäger and F. Vögtle, *Angew. Chem., Int. Ed.*, 1997, **36**, 930; (*e*) C. A. Hunter, *J. Am. Chem. Soc.*, 1992, **114**, 5303.
4 (*a*) K.-Y. Ng, A. R. Cowley and P. D. Beer, *Chem. Commun.*, 2006, 3676; (*b*) A. Caballero, F. Zapata, N. G. White, P. J. Costa, V. Félix and P. D. Beer, *Angew. Chem., Int. Ed.*, 2012, **51**, 1876.
5 (*a*) J.-P. Sauvage, *Acc. Chem. Res.*, 1998, **31**, 611 and references therein (*b*) J.-P. Collin, V. Heitz, S. Bonnet and J.-P. Sauvage, *Inorg. Chem. Commun.*, 2005, **8**, 1063; (*c*) J.-C. Chambron, J.-P. Collin, V. Heitz, D. Jouvenot, J.-M. Kern, P. Mobian, D. Pomeranc and J.-P. Sauvage, *Eur. J. Org. Chem.*, 2004, 1627; (*d*) M. Fujita, N. Fujita, K. Ogura and K. Yamaguchi, *Nature*, 1999, **400**, 52; (*e*) M. Chas, E. Pia, R. Toba, C. Peinador and J. M. Quintela, *Inorg. Chem.*, 2006, **45**, 6117; (*f*) T. S. M. Abedin, L. K. Thompson and D. O. Miller, *Chem. Commun.*, 2005, 5512; (*g*) C. P. McArdle, M. J. Irwin, M. C. Jennings, J. J. Vittal and R. J. Puddephatt, *Chem.–Eur. J.*, 2002, **8**, 723.
6 (*a*) J. E. Beves, B. A. Blight, C. J. Campbell, D. A. Leigh and R. T. McBurney, *Angew. Chem., Int. Ed.*, 2011, **50**, 9260; (*b*) R. Chakrabarty, P. S. Mukherjee and P. J. Stang, *Chem. Rev.*, 2011, **111**, 6810; (*c*) S. O. Scott, E. L. Gavey, S. J. Lind, K. C. Gordon and J. D. Crowley, *Dalton Trans.*, 2011, **40**, 12117; (*d*) J. E. M. Lewis, E. L. Gavey, S. A. Cameron and J. D. Crowley, *Chem. Sci.*, 2012, **3**, 778; (*e*) For an example of a Pt^{II} cage assembled under kinetic control see: O. Chepelin, J. Ujma, P. E. Barran and P. J. Lusby, *Angew. Chem., Int. Ed.*, 2012, **51**, 4194.
7 (*a*) V. Blanco, D. Abella, E. Pía, C. Platas-Iglesias, C. Peinador and J. M. Quintela, *Inorg. Chem.*, 2009, **48**, 4098; (*b*) C. Peinador, V. Blanco and J. M. Quintela, *J. Am. Chem. Soc.*, 2009, **131**, 920; (*c*) V. Blanco, M. Chas, D. Abella, C. Peinador and J. M. Quintela, *J. Am. Chem. Soc.*, 2007, **129**, 13978; (*d*) V. Blanco, A. Gutiérrez, C. Platas-Iglesias, C. Peinador and J. M. Quintela, *J. Org. Chem.*, 2009, **74**, 6577.
8 (*a*) C. Peinador, E. Pía, V. Blanco, M. D. García and J. M. Quintela, *Org. Lett.*, 2010, **12**, 1380; (*b*) V. Blanco, M. D. García, A. Terenzi, E. Pía, A. Fernández-Mato, C. Peinador and J. M. Quintela, *Chem.–Eur. J.*, 2010, **16**, 12373.
9 (*a*) V. Blanco, M. D. García, C. Peinador and J. M. Quintela, *Chem. Sci.*, 2011, **2**, 2407; (*b*) D. Abella, V. Blanco, E. Pía, M. Chas, C. Platas-Iglesias, C. Peinador and J. M. Quintela, *Chem. Commun.*, 2008, 2879.
10 (*a*) V. Blanco, M. Chas, D. Abella, E. Pía, C. Platas-Iglesias, C. Peinador and J. M. Quintela, *Org. Lett.*, 2008, **10**, 409; (*b*) M. Chas, D. Abella, V. Blanco, E. Pía, G. Blanco, A. Fernández, C. Platas-Iglesias, C. Peinador and J. M. Quintela, *Chem.–Eur. J.*, 2007, **13**, 8572.
11 The terminal OH group in the ethylene glycol chain is disordered in two positions.
12 (*a*) V. Balzani, A. Credi, S. J. Langford, J. F. Stoddart and M. Venturi, *Supramol. Chem.*, 2001, **13**, 303; (*b*) R. Ballardini, A. Credi, M. T. Gandolfini, C. Giansante, G. Marconi, S. Silvi and M. Venturi, *Inorg. Chim. Acta*, 2007, **360**, 1072.
13 P. Čudić, M. Žinić, V. Tomišić, V. Simeon, J.-P. Vigneronc and J.-M. Lehn, *J. Chem. Soc., Chem. Commun*, 1995, 1073.
14 (*a*) M. Liu, S. Li, M. Zhang, Q. Zhou, F. Wang, M. Hu, F. R. Fronczek, N. Li and F. Huang, *Org. Biomol. Chem.*, 2009, **7**, 1288; (*b*) T. Ikeda, M. Higuchi, A. Sato and D. G. Kurth, *Org. Lett.*, 2008, **10**, 2215.
15 E. M. López-Vidal, V. Blanco, M. D. García, C. Peinador and J. M. Quintela, *Org. Lett.*, 2012, **14**, 580.
16 P. R. Anelli, P. R. Ashton, R. Ballardini, V. Balzani, M. Delgado, M. T. Gandolfi, T. T. Goodnow, A. E. Kaifer, D. Philp, M. Pietraszkiewicz, L. Prodi, M. V. Reddington, A. M. Z. Slawin, N. Spencer, J. F. Stoddart, C. Vicent and D. J. Williams, *J. Am. Chem. Soc.*, 1992, **114**, 193.
17 D. B. Amabilino, P. L. Anelli, P. R. Ashton, G. R. Brown, E. Córdova, L. A. Godínez, W. Hayes, A. E. Kaifer, D. Philp, A. M. Z. Slawin, N. Spencer, J. F. Stoddart, M. S. Tolley and D. J. Williams, *J. Am. Chem. Soc.*, 1995, **117**, 11142.
18 M. Asakawa, P. R. Ashton, S. E. Boyd, C. L. Brown, R. E. Gillard, O. Kocian, F. M. Raymo, J. F. Stoddart, M. S. Tolley, A. J. P. White and D. J. Williams, *J. Org. Chem.*, 1997, **62**, 26.
19 D. B. Amabilino, P. R. Ashton, V. Balzani, S. E. Boyd, A. Credi, J. Y. Lee, S. Menzer, J. F. Stoddart, M. Venturi and D. J. Williams, *J. Am. Chem. Soc.*, 1998, **120**, 4295.
20 L. G. Longsworth, *J. Phys. Chem.*, 1960, **64**, 1914.
21 T. Megyes, H. Jude, T. Grósz, I. Bakó, R. Radnai, G. Tárkányi, G. Pálinkás and P. J. Stang, *J. Am. Chem. Soc.*, 2005, **127**, 10731.
22 (*a*) G. M. Sheldrick, *SHELX-97, An Integrated System for Solving and Refining Crystal Structures from Diffraction Data*, University of Göttingen, Germany, 1997; (*b*) G. M. Sheldrick, *Acta Crystallogr., Sect. A: Fundam. Crystallogr.*, 2008, **A64**, 112.
23 L. J. Farrugia, *J. Appl. Crystallogr.*, 1999, **32**, 837.
24 (*a*) A. L. Spek, *PLATON, A Multipurpose Crystallographic Tool*, Utrecht University, Utrecht, The Netherlands, 2008; (*b*) A. L. Spek, *Acta Crystallogr., Sect. D: Biol. Crystallogr.*, 2009, **D65**, 148.

